PFC/JA-88-21

NONLINEAR BOUND ON UNSTABLE FIELD ENERGY IN RELATIVISTIC ELECTRON BEAMS AND PLASMAS

Ronald C. Davidson
and
Peter H. Yoon

May, 1988

NONLINEAR BOUND ON UNSTABLE FIELD ENERGY IN RELATIVISTIC ELECTRON BEAMS AND PLASMAS

Ronald C. Davidson
Plasma Fusion Center
Massachusetts Institute of Technology, Cambridge, MA 02139

Peter H. Yoon
Center for Space Research
Massachusetts Institute of Technology, Cambridge, MA 02139

ABSTRACT

This paper makes use of Fowler's method [T.K. Fowler, J. Math. Phys. 4, 559 (1963)] to determine the nonlinear thermodynamic bound on field energy in unstable plasmas or electron beams in which the electrons are relativistic. Treating the electrons as the only active plasma component, the nonlinear Vlasov-Maxwell equations and the associated global conservation constraints are used to calculate the lowest upper bound on the field energy $[\Delta\mathcal{E}_F]_{MAX}$ that can evolve for general initial electron distribution function $f_{b0} \equiv f_b(\underset{\sim}{x},\underset{\sim}{p},0)$. The results are applied to three choices of initial distribution function f_{b0}. Two of the distribution functions have an inverted population in momentum $p_\perp$ perpendicular to the magnetic field $B_0\hat{\underset{\sim}{e}}_z$, and the third distribution function reduces to a bi-Maxwellian in the nonrelativistic limit. The lowest upper bound on the efficiency of radiation generation, $\eta_{MAX} = [\Delta\mathcal{E}_F]_{MAX}/[V^{-1}\int d^3x\int d^3p(\gamma - 1)mc^2 f_{b0}]$, is calculated numerically over a wide range of system parameters for varying degrees of initial anisotropy.

I. INTRODUCTION

More than two decades ago, Fowler[1,2] developed an elegant theoretical formalism for calculating nonlinear thermodynamic bounds on the field energy in unstable plasmas. In essence, the approach makes use of global conservation constraints satisfied by the nonlinear Vlasov-Maxwell equations to determine the lowest upper bound on the field energy $[\Delta\mathcal{E}_F]_{MAX}$ that can evolve for given initial distribution function $f(\underset{\sim}{x},\underset{\sim}{p},0)$. Over the years, this method,[1,2] or variations thereof, has been used to estimate nonlinear bounds on field energy for applications ranging from electromagnetic instabilities driven by energy anisotropy,[3] to shear-driven instabilities in nonneutral plasmas,[4] to anomalous electron energy transport in tokamaks,[5] to nonlinear bound estimates using both kinetic[6] and macroscopic[6,7] models of plasmas and classical fluids.

The present analysis extends Fowler's method[1,2] to the case of relativistic electrons, and the nonlinear bound on field energy $[\Delta\mathcal{E}_F]_{MAX}$ is calculated for several initial electron distribution functions $f_{b0} \equiv f_b(\underset{\sim}{x},\underset{\sim}{p},0)$ that incorporate an energy anisotropy or an inverted population in momentum $p_\perp$ perpendicular to an applied magnetic field $B_0\hat{\underset{\sim}{e}}_z$. There are several motivations for this work. First, various microwave generation devices[8] (such as gyrotrons, magnetrons, cyclotron autoresonance masers, etc.) make use of relativistic electrons interacting with a magnetic field to generate coherent radiation. The present analysis provides a framework to estimate the lowest upper bound on the efficiency η_{MAX} of radiation generation for particular choices of input beam distribution function f_{b0}. Second,

instabilities driven by relativistic electrons can play an important role in various space[9,10] and astrophysical[11-13] plasma applications. For example, one active area of study relates to coherent radiation emission from compact, accreting objects such as pulsars and active galactic nuclei in which the magnetic field is strong, and the electrons are anisotropic and relativistic ($T_e \lesssim 3000$ keV). Finally, calculations that model the detailed nonlinear dynamics of a particular instability usually make several restrictive assumptions, such as a fixed propagation direction, or that a single wave or type of instability dominates the nonlinear evolution. The present analysis, which is based on global conservation constraints satisfied by the nonlinear Vlasov-Maxwell equations, permits a lowest upper bound $[\Delta\mathcal{E}_F]_{MAX}$ to be placed on the field energy that evolves for general initial distribution function $f_b(\underset{\sim}{x},\underset{\sim}{p},0)$. The approach is insensitive to the particular instability (indeed, there may be several instabilities operating simultaneously) and the detailed nonlinear dynamics of the system.

As further background, there are numerous instabilities driven by electron energy anisotropy, or an inverted population in momentum $p_\perp$ perpendicular to the magnetic field $B_0\hat{\underset{\sim}{e}}_z$. For example, depending on the degree and direction of energy anisotropy, there are various classical Weibel-type instabilities[14] ranging from the electron whistler instability[15,16] for wave propagation parallel to $B_0\hat{\underset{\sim}{e}}_z$, to the ordinary-mode electromagnetic instability[17] for propagation perpendicular to $B_0\hat{\underset{\sim}{e}}_z$. On the other hand, for an inverted population in perpendicular momentum $p_\perp$, instabilities range from the electrostatic loss-cone

instability[18] to the cyclotron maser instability,[19-21] which is the basic instability mechanism for the cyclotron autoresonance maser (CARM) and the gyrotron.[8] A detailed review of the linear growth properties of many of these instabilities has been given by Davidson.[22]

The organization of this paper is the following. The theoretical model, which is based on the nonlinear Vlasov-Maxwell equations, is described in Sec. II. Treating the electrons as the only active plasma component, we make use of the global conservation constraints corresponding to the conservation of total energy, average number density, entropy, and total axial momentum, to obtain the formal expression in Eq.(16) for the upper bound on field energy $[\Delta\mathcal{E}_F]_{MAX}$ for general initial distribution function $f_{b0} = f_b(\underset{\sim}{x},\underset{\sim}{p},0)$. From Eqs.(15) and (16) it is evident that $\Delta\mathcal{E}_F(t)$ is bounded from above by the value $[\Delta\mathcal{E}_F]_{MAX}$ that would be achieved if $f_b(\underset{\sim}{x},\underset{\sim}{p},t)$ were to relax to the isotropic, drifting, relativistic thermal equilibrium distribution $g = \beta \exp\{-(\gamma mc^2 - V_b p_z)/T_b\}$. In Sec. III, the values of the constants β, V_b and T_b are chosen so as to <u>minimize</u> $[\Delta\mathcal{E}_F]_{MAX}$. This leads to the expression for $[\Delta\mathcal{E}_F]_{MAX}$ in Eq.(27), where β, V_b and T_b are determined in terms of the initial conditions from Eqs.(24)-(26). Finally, in Sec. IV, we apply the results in Sec. III to three choices of initial distribution function f_{b0}. Two of the distribution functions [Eqs.(35) and (38)] have an inverted population in perpendicular momentum $p_\perp$, and the third distribution function [Eq.(41)] reduces to a bi-Maxwellian in the nonrelativistic limit. The lowest upper bound on the efficiency of radiation generation, $\eta_{MAX} = [\Delta\mathcal{E}_F]_{MAX}/V^{-1}\int d^3x \int d^3p(\gamma - 1)mc^2 f_{b0}]$,

is calculated numerically over a wide range of system parameters for varying degrees of initial anisotropy.

Finally, we clarify the range of applicability of the analysis in Secs. II-IV, which treats the electrons as the only active plasma component. For applications to one-component electron plasmas, such as relativistic nonneutral electron beams used in microwave generation, the neglect of equilibrium electric and magnetic self fields necessarily requires that the beam density and current be low (tenuous-beam approximation). On the other hand, for applications to multi-component, charge-neutral plasmas, the neglect of positive ion dynamics ($m_i \to \infty$) necessarily implies that the analysis is restricted to high-frequency electron-driven instabilities.

II. ASSUMPTIONS AND THEORETICAL MODEL

The present analysis neglects positive ion dynamics ($m_i \to \infty$), but allows the electron motion to be relativistic. It is further assumed that perturbations are about a spatially uniform equilibrium with average density $\hat{n}_b$ = const. and uniform magnetic field $B_0\hat{e}_z$, and that the electron current and density are sufficiently low that equilibrium self fields can be neglected in describing the nonlinear evolution of the system. The electric and magnetic fields, $\underset{\sim}{E}(\underset{\sim}{x},t)$ and $\underset{\sim}{B}(\underset{\sim}{x},t)$, are expressed as

$$\underset{\sim}{E}(\underset{\sim}{x},t) = \delta\underset{\sim}{E}(\underset{\sim}{x},t) \ ,$$
$$\underset{\sim}{B}(\underset{\sim}{x},t) = B_0\hat{e}_z + \delta\underset{\sim}{B}(\underset{\sim}{x},t) \ , \tag{1}$$

and the electron distribution function $f_b(\underset{\sim}{x},\underset{\sim}{p},t)$ evolves according to the nonlinear Vlasov equation

$$\frac{\partial}{\partial t} f_b + \frac{\partial}{\partial \underset{\sim}{x}} \cdot \left(\underset{\sim}{v} f_b\right) - e \frac{\partial}{\partial \underset{\sim}{p}} \cdot \left[\left(\delta\underset{\sim}{E} + \frac{\underset{\sim}{v}\times(B_0\hat{e}_z + \delta\underset{\sim}{B})}{c}\right) f_b\right] = 0 \ . \tag{2}$$

Here, $\underset{\sim}{p}$ is the mechanical momentum, $\underset{\sim}{v} = \underset{\sim}{p}/\gamma m$ is the velocity, $\gamma = (1 + \underset{\sim}{p}^2/m^2c^2)^{1/2}$ is the relativistic mass factor, $-e$ is the electron charge, m is the electron rest mass, and c is the speed of light <u>in vacuo</u>. In Eq.(2), the field perturbations $\delta\underset{\sim}{E}(\underset{\sim}{x},t) = (\delta E_x, \delta E_y, \delta E_z)$ and $\delta\underset{\sim}{B}(\underset{\sim}{x},t) = (\delta B_x, \delta B_y, \delta B_z)$, which are allowed to have arbitrary polarization, are determined self-consistently in terms of $f_b(\underset{\sim}{x},\underset{\sim}{p},t)$ from Maxwell's equations.

To determine a nonlinear bound on the unstable field energy that can develop for given initial distribution function

$$f_{b0} = f_b(\underset{\sim}{x},\underset{\sim}{p},0) \ , \tag{3}$$

Fowler's method[1-3] makes use of global conservation constraints that are satisfied by the nonlinear Vlasov-Maxwell equations. For the configuration considered here, the obvious conserved quantities are: the total (particle plus field) energy (U), the average number density (N), the entropy (S), and the total (particle plus field) axial momentum (C_z). These constraint conditions can be expressed as

$$U = \int \frac{d^3x}{V} \left\{ \int d^3p \gamma mc^2 f_b + \frac{(\delta \underset{\sim}{E})^2 + (\delta \underset{\sim}{B})^2}{8\pi} \right\} = \text{const.}, \tag{4}$$

$$N = \int \frac{d^3x}{V} \int d^3p f_b = \text{const.}, \tag{5}$$

$$S = - \int \frac{d^3x}{V} \int d^3p f_b \ell n(f_b/\beta) = \text{const.}, \tag{6}$$

$$C_z = \int \frac{d^3x}{V} \left\{ \int d^3p p_z f_b + \frac{1}{4\pi c} \left(\delta E_x \delta B_y - \delta E_y \delta B_x \right) \right\} = \text{const.}, \tag{7}$$

where $V = L_x L_y L_z$, and the spatial integrations in Eqs.(4)-(7) are over the fundamental periodicity lengths of the perturbations. In Eq.(6), β is a (yet unspecified) positive constant. For smooth, differentiable $G(f_b)$, we also note that the generalized entropy $V^{-1} \int d^3x \int d^3p G(f_b)$ is exactly conserved (= const.) by the nonlinear Vlasov-Maxwell equation. The choice of entropy S in Eq.(6) is particularly convenient because it leads to a reference state corresponding to thermal equilibrium. Finally, in Eq.(5), it should be noted that the constant N can be identified with the average electron density ($N \equiv \hat{n}_b$).

We now make use of the global conservation constraints in Eqs.(4)-(7) to construct an effective Helmholtz free energy F defined by

$$F = U - V_b C_z - T_b S - T_b N \ , \tag{8}$$

where V_b and T_b are (yet unspecified) constants. Because F is a combination of conserved quantities, it follows that

$$F(t) = F(0) = \text{const.} \tag{9}$$

during the nonlinear evolution of the system. A convenient, positive-definite, quadratic measure of the field perturbations is

$$\mathcal{E}_F(t) = \frac{1}{8\pi} \int \frac{d^3x}{V} \left\{ (\delta E_x - \beta_b \delta B_y)^2 + (\delta E_y + \beta_b \delta B_x)^2 \right. \tag{10}$$

$$\left. + (\delta E_z)^2 + (1 - \beta_b^2)\left[(\delta B_x)^2 + (\delta B_y)^2\right] + (\delta B_z)^2 \right\} \ ,$$

where $\beta_b \equiv V_b/c$, and $\beta_b^2 < 1$ is assumed. Substituting Eqs.(4)-(7) into Eq.(8), and making use of Eq.(9), we solve for $\Delta\mathcal{E}_F(t) = \mathcal{E}_F(t) - \mathcal{E}_F(0)$. This gives

$$\Delta\mathcal{E}_F(t) = \int \frac{d^3x}{V} \int d^3p \left\{ -(\gamma mc^2 - V_b p_z)(f_b - f_{b0}) \right. \tag{11}$$

$$\left. - T_b\left[f_b \ell n(f_b/\beta) - f_{b0} \ell n(f_{b0}/\beta) - (f_b - f_{b0})\right] \right\} \ .$$

Equation (11) is an exact expression for $\Delta\mathcal{E}_F(t)$, valid as $f_b(\underset{\sim}{x},\underset{\sim}{p},t)$ evolves according to the nonlinear Vlasov-Maxwell equations from general initial condition $f_{b0} = f_b(\underset{\sim}{x},\underset{\sim}{p},0)$.

It is straightforward to show from Eq.(11) that $\Delta\mathcal{E}_F$ is a <u>maximum</u> whenever f_b corresponds to a relativistic thermal equilibrium distribution with temperature T_b and average axial velocity $V_b\hat{e}_z$. Taking the variation of $\Delta\mathcal{E}_F$ in Eq.(11) with respect to f_b and setting $\delta[\Delta\mathcal{E}_F] = 0$ gives

$$\delta(\Delta\mathcal{E}_F) = \int \frac{d^3x}{V} \int d^3p \left\{-(\gamma mc^2 - V_b p_z) - T_b \ell n(f_b/\beta)\right\}(\delta f_b) = 0 \ . \tag{12}$$

Equation (12) is satisfied provided

$$f_b = g = \beta \exp\left\{-(\gamma mc^2 - V_b p_z)/T_b\right\} \ . \tag{13}$$

For positive β and T_b, which we assume to be the case, Eq.(13) corresponds to a relativistic thermal equilibrium distribution drifting with axial velocity V_b along the applied magnetic field $B_0\hat{e}_z$. Taking the second variation of Eq.(12) with respect to f_b, and evaluating at $f_b = g$, we obtain

$$\delta[\delta(\Delta\mathcal{E}_F)] = -T_b \int \frac{d^3x}{V} \int d^3p \ \frac{(\delta f_b)^2}{g} \leq 0 \ . \tag{14}$$

It is therefore concluded that $\Delta\mathcal{E}_F$ is a <u>maximum</u> whenever $f_b = g$ in Eq.(11). That is, at any instant of time,

$$\Delta\mathcal{E}_F(t) \leq [\Delta\mathcal{E}_F]_{MAX} \ , \tag{15}$$

where

$$[\Delta\mathcal{E}_F]_{MAX} = \int \frac{d^3x}{V} \int d^3p \left\{(\gamma mc^2 - V_b p_z)(f_{b0} - g) + T_b\left[f_{b0}\ell n(f_{b0}/\beta) - g\ell n(g/\beta) + (g - f_{b0})\right]\right\} \ . \tag{16}$$

Stated another way, $\Delta\mathcal{E}_F(t)$ is bounded from above by the value $[\Delta\mathcal{E}_F]_{MAX}$ that would be achieved if f_b were to relax to the isotropic, drifting, thermal equilibrium distribution $g = \beta \exp\{-(\gamma mc^2 - V_b p_z)/T_b\}$. Substituting the expression for g into Eq.(16), the upper bound $[\Delta\mathcal{E}_F]_{MAX}$ can also be expressed as

$$[\Delta\mathcal{E}_F]_{MAX} = \int \frac{d^3x}{V} \int d^3p \left\{(\gamma mc^2 - V_b p_z) f_{b0} + T_b\left[f_{b0} \ell n(f_{b0}/\beta) + \left(\beta \exp\{-(\gamma mc^2 - V_b p_z)/T_b\} - f_{b0}\right)\right]\right\} . \tag{17}$$

III. LOWEST UPPER BOUND ON $[\Delta\mathcal{E}_F]_{MAX}$

Thus far, the parameters β, V_b and T_b in Eq.(17) [or Eq.(16)] have been arbitrary. To determine the lowest upper bound on $\Delta\mathcal{E}_F(t)$ consistent with the four conservation constraints in Eqs.(4)-(7), we now choose β, V_b and T so that $[\Delta\mathcal{E}_F]_{MAX}$ is a minimum.[1-3] The conditions $(\partial/\partial\beta)[\Delta\mathcal{E}_F]_{MAX} = 0$ and $(\partial/\partial V_b)[\Delta\mathcal{E}_F]_{MAX} = 0$ readily give

$$\int \frac{d^3x}{V} \int d^3p\ (g - f_{b0}) = 0\ , \tag{18}$$

and

$$\int \frac{d^3x}{V} \int d^3p p_z\ (g - f_{b0}) = 0\ , \tag{19}$$

respectively. Here, the reference distribution function g is defined in Eq.(13). Furthermore, the condition $(\partial/\partial T_b)[\Delta\mathcal{E}_F]_{MAX} = 0$ can be expressed as

$$\int \frac{d^3x}{V} \int d^3p \left(g\ell n(g/\beta) - f_{b0}\ell n(f_{b0}/\beta)\right) = 0\ , \tag{20}$$

where use has been made of Eq.(18) and $-(\gamma mc^2 - V_b p_z)(\beta/T_b) \times \exp\{-(\gamma mc^2 - V_b p_z)/T_b\} = g\ell n(g/\beta)$.

For specified initial distribution function f_{b0}, Eqs.(18)-(20) are used to determine those values of (β, V_b, T_b) that minimize the upper bound $[\Delta\mathcal{E}_F]_{MAX}$, i.e., that give the lowest estimate of $[\Delta\mathcal{E}_F]_{MAX}$ consistent with the four global conservation constraints in Eqs.(4)-(7). It should be noted that the conditions in Eqs.(18)-(20) are equivalent to the conditions for

conservation of particle number, axial momentum, and entropy, if $f_b(\underset{\sim}{x},\underset{\sim}{p},t)$ were to relax from the initial state f_{b0} to the reference state g. Substituting Eqs.(18)-(20) into Eq.(17), the estimate of $[\Delta\mathcal{E}_F]_{MAX}$ can be expressed in the equivalent form

$$[\Delta\mathcal{E}_F]_{MAX} = \int \frac{d^3x}{V} \int d^3p(\gamma-1)mc^2(f_{b0}-g) \ . \tag{21}$$

Keep in mind from the definition in Eq.(10) that $\Delta\mathcal{E}_F(t)$ is a quadratic measure of the change in field energy associated with the amplifying field perturbations (assuming that the initial state f_{b0} is unstable). Therefore, the condition $\Delta\mathcal{E}_F(t) \leq [\Delta\mathcal{E}_F]_{MAX}$, where $[\Delta\mathcal{E}_F]_{MAX}$ is defined in Eq.(21), is simply a statement that $\Delta\mathcal{E}_F(t)$ is bounded from above by the change in kinetic energy that would result if $f_b(\underset{\sim}{x},\underset{\sim}{p},t)$ were to relax from the initial state f_{b0} to the thermal equilibrium reference state g.

We return to the conditions in Eqs.(18)-(20), which determine the values of (β,V_b,T_b) that minimize $[\Delta\mathcal{E}_F]_{MAX}$ for specified initial state $f_{b0} = f_b(\underset{\sim}{x},\underset{\sim}{p},0)$. It is convenient to introduce the abbreviated notation

$$\hat{n}_b = \int \frac{d^3x}{V} \int d^3p f_{b0} \ ,$$

$$\hat{n}_b\hat{p}_{zb} = \int \frac{d^3x}{V} \int d^3p p_z f_{b0} \ , \tag{22}$$

where $\hat{n}_b$ = const. is the average electron density, and $\hat{p}_{zb}$ is the average particle momentum in the z-direction associated with the initial state f_{b0}. We further define

$$\gamma_b = \left(1 - V_b^2/c^2\right)^{-1/2},$$
$$\alpha_b = \frac{mc^2}{\gamma_b T_b}, \tag{23}$$

where α_b is a dimensionless parameter that measures the thermal spread in the reference state $g = \beta \exp\{-(\gamma mc^2 - V_b p_z)/T_b\}$. (For example, $\alpha_b << 1$ corresponds to an ultrarelativistic reference state with $\gamma_b T_b >> mc^2$). Making use of standard integral identities related to the drifting thermal equilibrium distribution function g, it can be shown that Eqs.(18) and (19) give

$$\beta = \frac{\hat{n}_b \alpha_b}{4\pi (mc)^3 \gamma_b K_2(\alpha_b)}, \tag{24}$$

and

$$\gamma_b m V_b \left[\frac{K_3(\alpha_b)}{K_2(\alpha_b)} - \frac{1}{\alpha_b} \right] = \hat{p}_{zb}, \tag{25}$$

respectively. Here, $K_n(x)$ is the modified Bessel function of the second kind of order n. Note that Eq.(24) relates the normalization constant β that occurs in the definition of the reference state g to the constant $\alpha_b = mc^2/\gamma_b T_b$ and the average density $\hat{n}_b$. On the other hand, Eq.(25) relates the axial momentum $\gamma_b m V_b$ of the reference state g to the constant α_b and the axial momentum $\hat{p}_{zb}$ of the initial state f_{b0}. Finally, the entropy constraint in Eq.(20) can be expressed as

$$\alpha_b \left[\frac{K_3(\alpha_b)}{K_2(\alpha_b)} - \frac{1}{\alpha_b} \right] - \ell n \beta = - \frac{1}{\hat{n}_b} \int \frac{d^3x}{V} \int d^3p f_{b0} \ell n f_{b0}, \tag{26}$$

which relates α_b and β to the entropy of the initial state f_{b0}.

To summarize, for specified initial distribution function $f_{b0} = f_b(\underset{\sim}{x},\underset{\sim}{p},0)$, the ancillary constraints in Eqs.(24)-(26) are used to calculate (numerically) the values of β, V_b and $\alpha_b = mc^2/\gamma_b T_b$ that minimize the upper bound $[\Delta\mathscr{E}_F]_{MAX}$ associated with the energy of the field perturbations. After some algebraic manipulation that makes use of Eqs.(13), (21), (24) and (25), we find that the $[\Delta\mathscr{E}_F]_{MAX}$ can be expressed in the equivalent form

$$[\Delta\mathscr{E}_F]_{MAX} = \int \frac{d^3x}{V} \int d^3p \left\{(\gamma - 1)mc^2 f_{b0} - \gamma_b mc^2 \left[\frac{K_3(\alpha_b)}{K_2(\alpha_b)} - \frac{1}{\alpha_b} - \frac{1}{\gamma_b} \right] f_{b0} \right\} , \tag{27}$$

where $V^{-1}\int d^3x \int d^3p f_{b0} = \hat{n}_b = V^{-1}\int d^3x \int d^3p g$. As a general remark, if $[\Delta\mathscr{E}_F]_{MAX}$ defined in Eq.(27) is non-positive for a particular choice of $f_b(\underset{\sim}{x},\underset{\sim}{p},0)$, then we conclude that $\Delta\mathscr{E}_F(t)$ cannot increase from its initial value and the system is <u>stable</u>.

A simple check on Eqs.(24)-(27) can be obtained in the nonrelativistic limit where $\gamma_b \to 1$ and $\alpha_b = mc^2/\gamma_b T_b >> 1$. For example, let us assume that $\hat{p}_{zb} = 0$, and make use of $K_2(\alpha_b) \simeq (\pi/2\alpha_b)^{1/2} \exp(-\alpha_b)$ and $K_3(\alpha_b)/K_2(\alpha_b) \simeq 1 + 5/(2\alpha_b)$ for $\alpha_b >> 1$. We then obtain for $\hat{p}_{zb} = 0$ and $\alpha_b >> 1$

$$\beta = \frac{\hat{n}_b}{(2\pi m T_b)^{3/2}} \exp\left(\frac{mc^2}{T_b}\right) ,$$

$$V_b = 0 , \tag{28}$$

$$T_b = \frac{\hat{n}_b^{2/3}}{2\pi m} \exp\left\{-1 - \frac{2}{3\hat{n}_b}\left[\int \frac{d^3x}{V} \int d^3p f_{b0} \ell n f_{b0}\right]\right\} .$$

In the nonrelativistic limit where $(\gamma - 1)mc^2 \simeq \underset{\sim}{p}^2/2m$, the reference state is $g = \hat{n}_b(2\pi m T_b)^{-3/2} \exp(-\underset{\sim}{p}^2/2mT_b)$, and the nonlinear bound in Eq.(27) reduces to

$$[\Delta \mathcal{E}_F]_{MAX} = \int \frac{d^3x}{V} \int d^3p \left(\frac{\underset{\sim}{p}^2}{2m} - \frac{3}{2} T_b \right) f_{b0} \cdot \tag{29}$$

Equations (28) and (29) are the expected results in the nonrelativistic regime,[1-3] and can be used to estimate $[\Delta \mathcal{E}_F]_{MAX}$ for various choices of initial state f_{b0}, such as bi-Maxwellian and loss-cone distribution functions.

IV. CALCULATION OF NONLINEAR BOUNDS

Equation (27) can be used to calculate $[\Delta\mathcal{E}_F]_{MAX}$ for a wide range of initial distribution functions $f_{b0} = f_b(\underset{\sim}{x},\underset{\sim}{p},0)$. For specified f_{b0}, the ancillary constraints in Eqs.(24)-(26) determine the values of β, V_b and $\alpha_b = mc^2/\gamma_b T_b$ that minimize $[\Delta\mathcal{E}_F]_{MAX}$ consistent with the global conservation constraints in Eqs.(4)-(7). In this section, we consider three choices of initial distribution function f_{b0} for which a numerical evaluation of $[\Delta\mathcal{E}_F]_{MAX}$ is tractable. Two of the distribution functions [Eqs.(35) and (38)] have an inverted population in perpendicular momentum $p_\perp$, and the third distribution function [Eq.(41)] reduces to a bi-Maxwellian in the nonrelativistic limit.

For simplicity, we specialize to the case where $\hat{p}_{zb} = \hat{n}_b^{-1}V^{-1}\int d^3x\int d^3p\, p_z f_{b0} = 0$, corresponding to zero average axial momentum at $t = 0$. For a one-component electron plasma, this is equivalent to evaluating $[\Delta\mathcal{E}_F]_{MAX}$ in a frame of reference moving with the axial velocity of the initial distribution function. Setting $\hat{p}_{zb} = 0$ in Eq.(25) gives

$$V_b = 0 \ , \qquad \gamma_b = 1 \ , \tag{30}$$

and Eqs.(24) and (26) can be expressed as

$$\beta(mc)^3 = \frac{\hat{n}_b\alpha_b}{4\pi K_2(\alpha_b)} \ , \tag{31}$$

and

$$\alpha_b\left[\frac{K_3(\alpha_b)}{K_2(\alpha_b)} - \frac{1}{\alpha_b}\right] = -\frac{1}{\hat{n}_b}\int\frac{d^3x}{V}\int d^3p f_{b0}\ell n(f_{b0}/\beta) \ , \qquad (32)$$

where $\alpha_b = mc^2/T_b$ and $\gamma_b = 1$. It is also convenient to measure $[\Delta\mathcal{E}_F]_{MAX}$ in units of the initial kinetic energy density $V^{-1}\int d^3x\int d^3p(\gamma - 1)mc^2 f_{b0}$. We therefore introduce the quantity η_{MAX} defined by

$$\eta_{MAX} = \frac{[\Delta\mathcal{E}_F]_{MAX}}{V^{-1}\int d^3x\int d^3p(\gamma - 1)mc^2 f_{b0}} \ . \qquad (33)$$

Equations (27) and (33) then give

$$\eta_{MAX} = 1 - \hat{n}_b mc^2\left[\frac{K_3(\alpha_b)}{K_2(\alpha_b)} - \frac{1}{\alpha_b} - 1\right] \times \left[\int\frac{d^3x}{V}\int d^3p(\gamma - 1)mc^2 f_{b0}\right]^{-1} , \qquad (34)$$

where use has been made of $\gamma_b = 1$ and the normalization condition $\hat{n}_b = V^{-1}\int d^3x\int d^3p f_{b0}$. Note that η_{MAX} defined in Eqs.(33) and (34) represents a lowest upper bound on the efficiency of radiation generation for specified initial distribution function f_{b0}.

A. Distribution Functions with Inverted Population in Perpendicular Momentum

As a first example, we consider perturbations about the distribution function

$$f_{b0} = \frac{\hat{n}_b\Theta(p_z^2 - \Delta_z^2)[\Theta(p_\perp - \hat{p}) - \Theta(p_\perp - \hat{p} + \Delta_\perp)]}{2\pi(mc)^3(\Delta_z/mc)(\Delta_\perp/mc)(2\hat{p}/mc - \Delta_\perp/mc)} \ , \qquad (35)$$

which has an inverted population in perpendicular momentum $p_\perp$ (Fig. 1). Here, $\hat{p}$, Δ_z, and $\Delta_\perp (\lesssim \hat{p})$ are positive constants, and $\Theta(x)$ is the Heaviside step function defined by $\Theta(x) = +1$ for $x < 0$, and $\Theta(x) = 0$ for $x > 0$. The normalization of f_{b0} in Eq.(35) is $V^{-1}\int d^3x \int d^3p f_{b0} = \hat{n}_b$. It is evident from Eq.(35) and Fig. 1 that f_{b0} corresponds to a rectangular 'water-bag' distribution in momentum space, revolved about the p_z-axis, with $f_{b0} = $ const. for $-\Delta_z < p_z < \Delta_z$ and $\hat{p} - \Delta_\perp < p_\perp < \hat{p}$, and $f_{b0} = 0$ outside of this region. That is, Eq.(35) incorporates a spread ($2\Delta_z$) in axial momentum p_z, and a spread ($\Delta_\perp$) in perpendicular momentum $p_\perp$.

Depending on the values of Δ_z and $\Delta_\perp$, it is well known that the distribution function f_{b0} in Eq.(35) has sufficient free energy to drive a variety of collective instabilities,[22] thereby resulting in an increase in $\Delta\mathcal{E}_F(t)$. These instabilities range from the electron whister[15,16] and cyclotron maser[19-21] instabilities for wave propagation along $B_0\hat{e}_z$, to electrostatic loss-cone[18] and ordinary-mode[17] Weibel instabilities for propagation perpendicular to $B_0\hat{e}_z$. To evaluate η_{MAX} for the choice of f_{b0} in Eq.(35), we first determine the entropy associated with the initial state. This gives

$$-\int \frac{d^3x}{V} \int d^3p f_{b0} \ell n(f_{b0}/\beta)$$

$$= -\hat{n}_b \ell n \left[\frac{\hat{n}_b/(mc)^3\beta}{2\pi(\Delta_z/mc)(\Delta_\perp/mc)(2\hat{p}/mc - \Delta_\perp/mc)} \right] . \tag{36}$$

Using Eq.(31) to eliminate β in Eq.(36), and substituting Eq.(36) into Eq.(32), we obtain

$$\frac{2K_2(\alpha_b)}{\alpha_b}\exp\left[\frac{\alpha_b K_3(\alpha_b)}{K_2(\alpha_b)} - 1\right] = \left(\frac{\Delta_z}{mc}\right)\left(\frac{\Delta_\perp}{mc}\right)\left(\frac{2\hat{p}}{mc} - \frac{\Delta_\perp}{mc}\right) . \tag{37}$$

For specified values of Δ_z/mc, $\Delta_\perp/mc$ and $\hat{p}/mc$ associated with the initial state f_{b0}, Eq.(37) constitutes a closed, transcendental equation that determines the corresponding value of $\alpha_b = mc^2/T_b$ associated with the reference state g. Once α_b is determined (numerically) from Eq.(37), then Eq.(34) is used to calculate η_{MAX} for the choice of f_{b0} in Eq.(35).

Following this procedure, we have made use of Eqs.(34), (35) and (37) to evaluate η_{MAX} over a wide range of system parameters. Typical numerical results are summarized in Figs. 2-4. Shown in Fig. 2 are plots of η_{MAX} versus $\Delta_\perp/\hat{p}$ obtained from Eq.(34) for fixed $\hat{p}/mc = 1.732$, and values of $\Delta_z/\Delta_\perp$ ranging from 0.05 to 1. As expected, η_{MAX} decreases as $\Delta_\perp/\hat{p}$ is increased, which corresponds to filling in the 'hole' in $p_\perp$-space. What is most striking in Fig. 2 is the significant decrease in η_{MAX} as the anisotropy factor $\Delta_z/\Delta_\perp$ is increased from small values. For example, for $\Delta_\perp/\hat{p} = 0.5$, η_{MAX} decreases from $\eta_{MAX} = 0.92$ for $\Delta_z = 0.05$, to $\eta_{MAX} = 0.53$ for $\Delta_z/\Delta_\perp = 1$. Evidently, an increase in axial momentum spread Δ_z can greatly reduce the maximum efficiency η_{MAX}. This is also consistent with the fact that estimates of linear growth rates (e.g., for the electron whistler and cyclotron maser instabilities) tend to decrease as the axial momentum spread increases. On the other hand, if the anisotropy is increased further to the region $\Delta_z/\Delta_\perp > 1$, there is additional

free energy again available to drive instability (such as the ordinary-mode Weibel instability[17] for wave propagation perpendicular to $B_0\hat{e}_z$). This is illustrated in Fig. 4, where η_{MAX} obtained from Eq.(34) is plotted versus $\Delta_z/\Delta_\perp$ for fixed ratios $\hat{p}/mc = 1.732$ and $\Delta_\perp/\hat{p} = 1$. Evidently, the estimate of η_{MAX} in Fig. 4 increases from $\eta_{MAX} = 0.27$ for $\Delta_z/\Delta_\perp = 1$, to $\eta_{MAX} = 0.64$ for $\Delta_z/\Delta_\perp = 5$. Finally, shown in Fig. 4 are plots of η_{MAX} versus $\Delta_\perp/\hat{p}$ obtained from Eq.(34) for fixed ratio $\Delta_z/\Delta_\perp = 1$, and values of $\hat{p}/mc$ ranging from 1.732 to 50. It is evident from Fig. 4 that η_{MAX} decreases slowly as $\hat{p}/mc$ is increased. That is, even though $[\Delta\mathcal{E}_F]_{MAX}$ increases in absolute magnitude, the fraction of initial kinetic energy available for conversion to unstable field energy decreases slowly as $\hat{p}/mc$ is increased [see the definition of η_{MAX} in Eq.(33)].

As a second example of a distribution function with inverted population in perpendicular momentum $p_\perp$, we briefly consider the case where f_{b0} is specified by

$$f_{b0} = \frac{3\hat{n}_b\Theta[(p_\perp^2 + p_z^2)^{1/2} - \hat{p}]\Theta(\hat{p} - \Delta_\perp - p_\perp)}{4\pi(mc)^3(\Delta_\perp/mc)^{3/2}(2\hat{p}/mc - \Delta_\perp/mc)^{3/2}} , \qquad (38)$$

where $\hat{p}$ and $\Delta_\perp$ ($\lesssim \hat{p}$) are positive constants. As illustrated in Fig. 5, the choice of distribution function in Eq.(35) corresponds to a uniform-density sphere in momentum space, subtracting out a cylinder of radius $p_\perp = \hat{p} - \Delta_\perp$ revolved about the p_z-axis. Unlike Eq.(35), we note from Eq.(38) and Fig. 5 that the axial momentum spread and the perpendicular momentum spread cannot be varied independently. Evaluating the entropy associated with f_{b0} in Eq.(38), we obtain

$$- \int \frac{d^3x}{V} \int d^3p f_{b0} \ell n(f_{b0}/\beta)$$

$$= -\hat{n}_b \ell n \left[\frac{3\hat{n}_b/(mc)^3\beta}{4\pi(\Delta_\perp/mc)^{3/2}(2\hat{p}/mc - \Delta_\perp/mc)^{3/2}} \right] . \tag{39}$$

Using Eq.(31) to eliminate β in Eq.(39), and substituting Eq.(39) into Eq.(32), we obtain

$$\frac{3K_2(\alpha_b)}{\alpha_b} \exp\left[\frac{\alpha_b K_3(\alpha_b)}{K_2(\alpha_b)} - 1 \right]$$

$$= \left(\frac{\Delta_\perp}{mc} \right)^{3/2} \left(\frac{2\hat{p}}{mc} - \frac{\Delta_\perp}{mc} \right)^{3/2} . \tag{40}$$

For specified values of $\Delta_\perp/mc$ and $\hat{p}/mc$, Eq.(40) can be used to determine the corresponding value of $\alpha_b = mc^2/T_b$. As before, once α_b is determined, Eq.(34) is used to evaluate η_{MAX} for the choice of f_{b0} in Eq.(38).

Typical numerical results obtained from Eqs.(34), (38) and (40) are summarized in Fig. 6, where η_{MAX} is plotted versus $\Delta_\perp/\hat{p}$, for values of $\hat{p}/mc$ ranging from 1.732 to 50. The qualitative behavior in Fig. 6 is similar to that in Figs. 2 and 4, i.e., η_{MAX} decreases with increasing values of $\Delta_\perp/\hat{p}$ and $\hat{p}/mc$.

B. Bi-Maxwellian Distribution Function

As a final example, we consider the case where f_{b0} is specified by

$$f_{b0} = \frac{\hat{n}_b \alpha_\perp}{4\pi(mc)^3 K_2(\alpha_z)} \exp\{-\alpha_\perp \gamma - (\alpha_z - \alpha_\perp)\gamma_z\}$$

$$\times \left[1 + \left(\frac{\alpha_z}{\alpha_\perp} - 1 \right) \frac{K_1(\alpha_z)}{\alpha_z K_2(\alpha_z)} \right]^{-1} , \tag{41}$$

where $\alpha_\perp = mc^2/T_\perp$, $\alpha_z = mc^2/T_z$, $\gamma = (1 + p_\perp^2/m^2c^2 + p_z^2/m^2c^2)^{1/2}$, and $\gamma_z = (1 + p_z^2/m^2c^2)^{1/2}$. The normalization of f_{b0} in Eq.(41) is $V^{-1}\int d^3x \int d^3p f_{b0} = \hat{n}_b$, and in the nonrelativistic regime ($\alpha_z >> 1$ and $\alpha_\perp >> 1$) Eq.(41) reduces to the familiar bi-Maxwellian distribution $f_{b0} = \hat{n}_b(2\pi m T_\perp)^{-1}(2\pi m T_z)^{-1/2} \exp\{-p_\perp^2/2mT_\perp - p_z^2/2mT_z\}$. Moreover, for isotropic plasma with $\alpha_\perp = \alpha_z$, Eq.(41) reduces to the thermal equilibrium distribution $f_{b0} = \text{const.} \exp(-\alpha_\perp\gamma)$, which we expect to be stable, with no free energy available to drive instability. Note that Eq.(41) does <u>not</u> have an inverted population in perpendicular momentum $p_\perp$. However, depending on the degree of anisotropy $T_z/T_\perp$, Eq.(41) is susceptible to various Weibel-type instabilities,[14,22] such as the electron whistler[15,16] and ordinary-mode[17] electromagnetic instabilities.

The procedure for calculating η_{MAX} for the choice of f_{b0} in Eq.(41) is analogous to that followed in Sec. IV.A. Evaluating the entropy associated with f_{b0} in Eq.(41), we obtain

$$-\int \frac{d^3x}{V} \int d^3p f_{b0} \ell n(f_{b0}/\beta)$$

$$= -\hat{n}_b \ell n \left\{ \frac{\alpha_\perp \hat{n}_b}{4\pi(mc)^3 \beta K_2(\alpha_z)} \left[1 + \left(\frac{\alpha_z}{\alpha_\perp} - 1 \right) \frac{K_1(\alpha_z)}{\alpha_z K_2(\alpha_z)} \right]^{-1} \right\} \qquad (42)$$

$$+\hat{n}_b \left\{ 1 + \left[1 + \frac{\alpha_z}{\alpha_\perp} + \frac{\alpha_z K_1(\alpha_z)}{K_2(\alpha_z)} \right] \left[1 + \left(\frac{\alpha_z}{\alpha_\perp} - 1 \right) \frac{K_1(\alpha_z)}{\alpha_z K_2(\alpha_z)} \right]^{-1} \right\} .$$

Using Eq.(31) to eliminate β in Eq.(42), and substituting Eq.(42) into Eq.(32), we obtain

$$\frac{K_2(\alpha_b)}{\alpha_b} \exp\left\{\frac{\alpha_b K_3(\alpha_b)}{K_2(\alpha_b)} - 2\right\}$$

$$= \frac{K_2(\alpha_z)}{\alpha_\perp}\left[1 + \left(\frac{\alpha_z}{\alpha_\perp} - 1\right)\frac{K_1(\alpha_z)}{\alpha_z K_2(\alpha_z)}\right] \qquad (43)$$

$$\times \exp\left\{\left[1 + \frac{\alpha_z}{\alpha_\perp} + \frac{\alpha_z K_1(\alpha_z)}{K_2(\alpha_z)}\right]\left[1 + \left(\frac{\alpha_z}{\alpha_\perp} - 1\right)\frac{K_1(\alpha_z)}{\alpha_z K_2(\alpha_z)}\right]^{-1}\right\} .$$

For specified values of $\alpha_z = mc^2/T_z$ and $\alpha_\perp = mc^2/T_\perp$, Eq.(43) can be used to determine the corresponding value of $\alpha_b = mc^2/T_b$. As before, once α_b is determined, Eq.(34) is used to evaluate η_{MAX} for the choice of f_{b0} in Eq.(41).

Typical numerical results obtained from Eqs.(34), (41) and (43) are summarized in Fig. 7. Here, η_{MAX} is plotted versus $T_z/T_\perp$ for two values of $\alpha_\perp = mc^2/T_\perp$, including $\alpha_\perp = 50$ (nonrelativistic regime) and $\alpha_\perp = 0.05$ (relativistic regime). A striking feature of Fig. 7 is that the normalized measure η_{MAX} of the bound on field energy [see definition of η_{MAX} in Eq.(33)] is very similar in the nonrelativistic ($\alpha_\perp = 50$) and highly relativistic ($\alpha_\perp = 0.05$) regimes. Also, as expected, when $T_z/T_\perp = \alpha_\perp/\alpha_z = 1$, the distribution function f_{b0} in Eq.(41) corresponds to an isotropic thermal equilibrium distribution, and no free energy is available to drive instability. Therefore, $\eta_{MAX} = 0$ for $T_z/T_\perp = 1$ in Fig. 7.

V. CONCLUSIONS

Treating the electrons as the only active plasma component, in Sec. II we made use of the global conservation constraints corresponding to the conservation of total energy, average number density, entropy, and total axial momentum, to obtain the formal expression in Eq.(16) for the upper bound on field energy $[\Delta\hat{\mathcal{E}}_F]_{MAX}$ for general initial distribution function $f_{b0} \equiv f_b(\underset{\sim}{x},\underset{\sim}{p},0)$. From Eqs.(15) and (16) it is evident that $\Delta\hat{\mathcal{E}}_F(t)$ is bounded from above by the value $[\Delta\hat{\mathcal{E}}_F]_{MAX}$ that would be achieved if $f_b(\underset{\sim}{x},\underset{\sim}{p},t)$ were to relax to the relativistic thermal equilibrium distribution $g = \beta \exp\{-(\gamma mc^2 - V_b p_z)/T_b\}$. In Sec. III, the values of the constants β, V_b and T_b were chosen so as to minimize $[\Delta\hat{\mathcal{E}}_F]_{MAX}$. This led to the expression for $[\Delta\hat{\mathcal{E}}_F]_{MAX}$ in Eq.(27), where β, V_b and T_b are determined in terms of the initial conditions from Eqs.(24)-(26). Finally, in Sec. IV, we applied the results in Sec. III to three choices of initial distribution function f_{b0}. Two of the distribution functions [Eqs.(35) and (38)] have an inverted population in perpendicular momentum $p_\perp$, and the third distribution function [Eq.(41)] reduces to a bi-Maxwellian in the nonrelativistic limit. The lowest upper bound on the efficiency of radiation generation, $\eta_{MAX} = [\Delta\hat{\mathcal{E}}_F]_{MAX}/V^{-1}\int d^3x \int d^3p(\gamma - 1)mc^2 f_{b0}]$, was calculated numerically over a wide range of system parameters for varying degrees of initial anisotropy. As a general remark, it is found that the normalized measure η_{MAX} of the bound on field energy is relatively insensitive to the initial kinetic energy $V^{-1}\int d^3x \int d^3p(\gamma - 1)mc^2 f_{b0}$ [see Figs. 4, 6, and 7].

As a final point, for specified initial distribution function f_{b0}, it should be emphasized that there is no a priori reason to anticipate that the field energy $\Delta\mathcal{E}_F(t)$ actually grows to the level $[\Delta\mathcal{E}_F]_{MAX}$ defined in Eq.(27). Rather, the present analysis shows that $\Delta\mathcal{E}_F(t)$ never exceeds the value $[\Delta\mathcal{E}_F]_{MAX}$ in Eq.(27), appropriately minimized by the conditions in Eqs.(24)-(26). Indeed, the actual maximum value of $\Delta\mathcal{E}_F(t)$ achieved for specified f_{b0} could be much lower than that in Eq.(27). As a general remark, if there are global conservation constraints in addition to those in Eqs.(4)-(7), then the inclusion of these additional constraints in the analysis will reduce the estimate of the nonlinear bound $[\Delta\mathcal{E}_F]_{MAX}$ even further.[3]

ACKNOWLEDGMENTS

This research was supported by the Office of Naval Research.

VI. REFERENCES

1. T.K. Fowler, J. Math. Phys. 4, 559 (1963).
2. T.K. Fowler, in Advances in Plasma Physics (Eds., A. Simon and W.B. Thompson, Interscience, 1968), Vol. 1, p. 201.
3. R.C. Davidson and S.T. Tsai, J. Plasma Phys. 9, 101 (1973).
4. R.C. Davidson, J. Plasma Phys. 33, 157 (1985).
5. T. Yamagishi, J. Plasma Phys. 36, 281 (1986).
6. D.D. Holm, J.E. Marsten, T. Ratiu and A. Weinstein, Physics Reports 123, 1 (1985).
7. H.D.I. Abarbanel, D.D. Holm, J.E. Marsten and T. Ratiu, Phil. Trans. Roy. Soc. (London) Ser. A318, 349 (1986).
8. See, for example, High-Power Microwave Sources (Eds., V. Granatstein and I. Alexeff, Artech House, 1987).
9. H.K. Wong, C.S. Wu and J.D. Gaffey, Jr., Phys. Fluids 28, 2751 (1985).
10. P.L. Pritchett, Phys. Fluids 29, 2919 (1986).
11. S.L. Shapiro and S.A. Teukolsky, Black Holes, White Dwarfs and Neutron Stars (Interscience, 1983).
12. M.J. Rees, Physica Scripta 17, 193 (1978).
13. R.D. Blandford and R.L. Znajek, Mon. Not. R. Astron. Soc. 179, 433 (1977).
14. E.S. Weibel, Phys. Rev. Lett. 2, 83 (1959).
15. R.N. Sudan, Phys. Fluids 6, 57 (1963).
16. C.F. Kennel and H.E. Petscheck, J. Geophys. Res. 72, 3303 (1967).
17. R.C. Davidson and C.S. Wu, Phys. Fluids 13, 1407 (1970).
18. R.A. Dory, G.E. Guest and E.G. Harris, Phys. Rev. Lett. 14, 131 (1965).

19. K.R. Chu and J.L. Hirschfield, Phys. Fluids 21, 461 (1978).

20. H.S. Uhm, R.C. Davidson and K.R. Chu, Phys. Fluids 21, 1866 (1978).

21. P.H. Yoon and R.C. Davidson, Phys. Rev. A35, 2619 (1987).

22. R.C. Davidson, in Handbook of Plasma Physics (Eds., M.N. Rosenbluth and R.Z. Sagdeev, North Holland, New York, 1983), Vol. 1, pp. 521-585.

FIGURE CAPTIONS

Fig. 1. Schematic of the distribution function $f_{b0}(p_\perp^2, p_z)$ defined in Eq.(35).

Fig. 2. Plots of η_{MAX} versus $\Delta_\perp/\hat{p}$ obtained from Eq.(34) for fixed $\hat{p}/mc = 1.732$, and values of $\Delta_z/\Delta_\perp$ ranging from 0.05 to 1, for the choice of distribution function f_{b0} in Eq.(35).

Fig. 3. Plots of η_{MAX} versus $\Delta_z/\Delta_\perp$ obtained from Eq.(34) for fixed $\hat{p}/mc = 1.732$ and $\Delta_\perp/\hat{p} = 1$ for the choice of distribution function f_{b0} in Eq.(35).

Fig. 4. Plots of η_{MAX} versus $\Delta_\perp/\hat{p}$ obtained from Eq.(34) for fixed $\Delta_z/\Delta_\perp = 1$, and values of $\hat{p}/mc$ ranging from 1.732 to 50, for the choice of distribution function f_{b0} in Eq.(35).

Fig. 5. Schematic of the distribution function $f_{b0}(p_\perp^2, p_z)$ defined in Eq.(38).

Fig. 6. Plots of η_{MAX} versus $\Delta_\perp/\hat{p}$ obtained from Eq.(34) for values of $\hat{p}/mc$ ranging from 1.732 to 50, for the choice of distribution function f_{b0} in Eq.(38).

Fig. 7. Plots of η_{MAX} versus $T_z/T_\perp$ obtained from Eq.(34) for $\alpha_\perp = mc^2/T_\perp = 50$ (solid curve) and $\alpha_\perp = 0.05$ (dashed curve), for the choice of distribution function f_{b0} in Eq.(41).

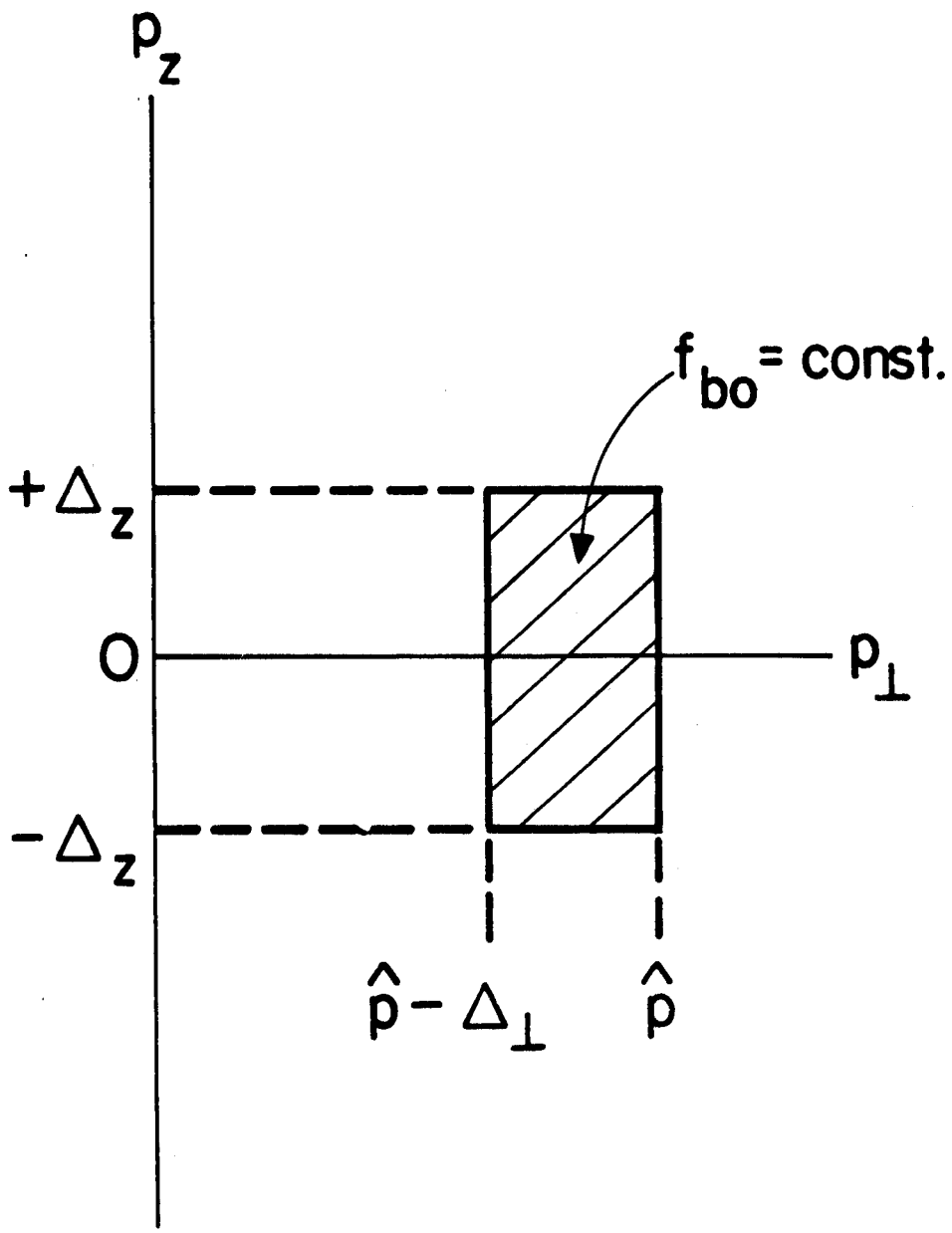

Fig. 1

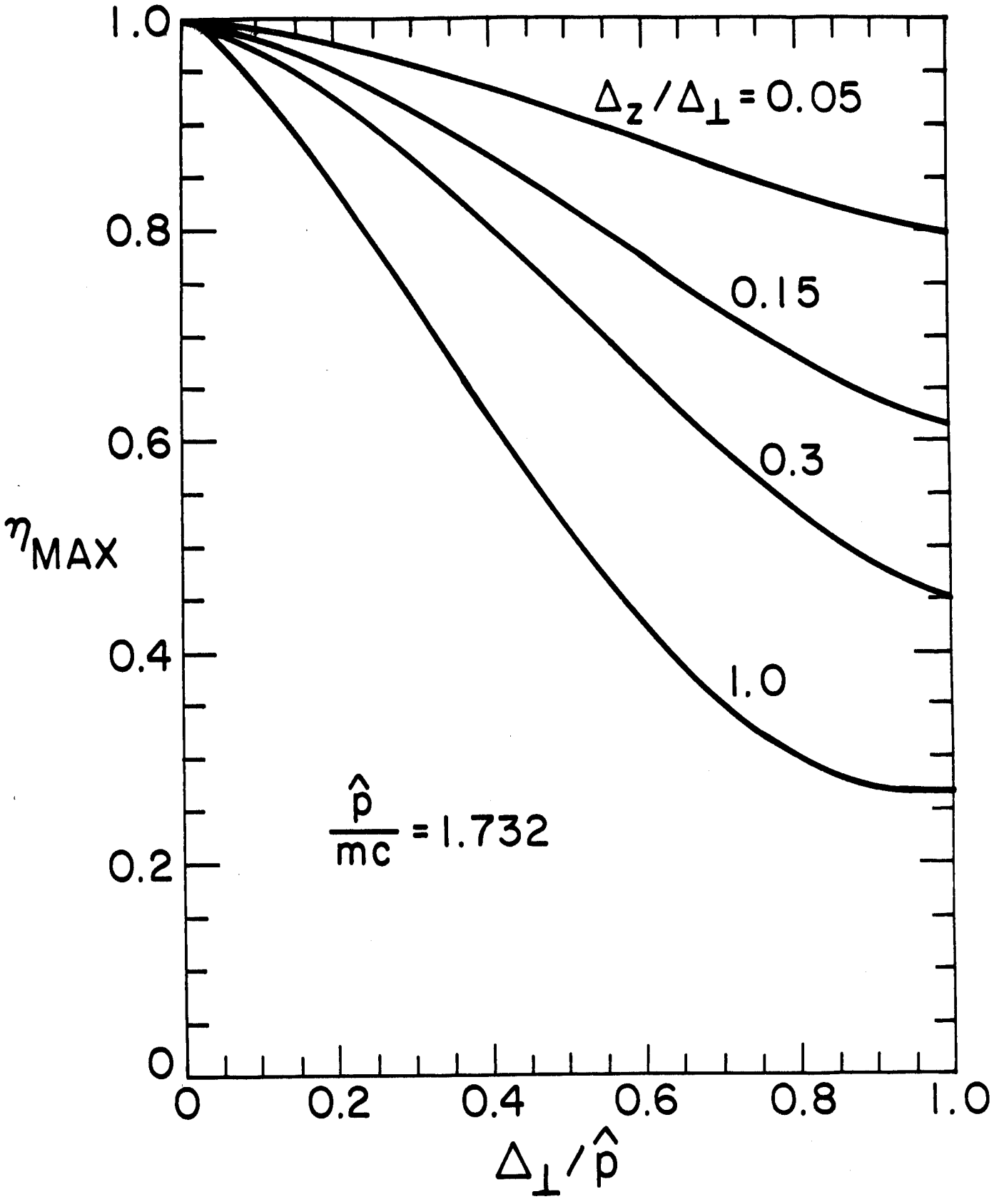
1.0
0.8
0.6
0.4
0.2
0
η_{MAX}
$\Delta_z/\Delta_\perp = 0.05$
0.15
0.3
1.0
$\frac{\hat{p}}{mc} = 1.732$
0
0.2
0.4
0.6
0.8
1.0
$\Delta_\perp/\hat{p}$

Fig. 2

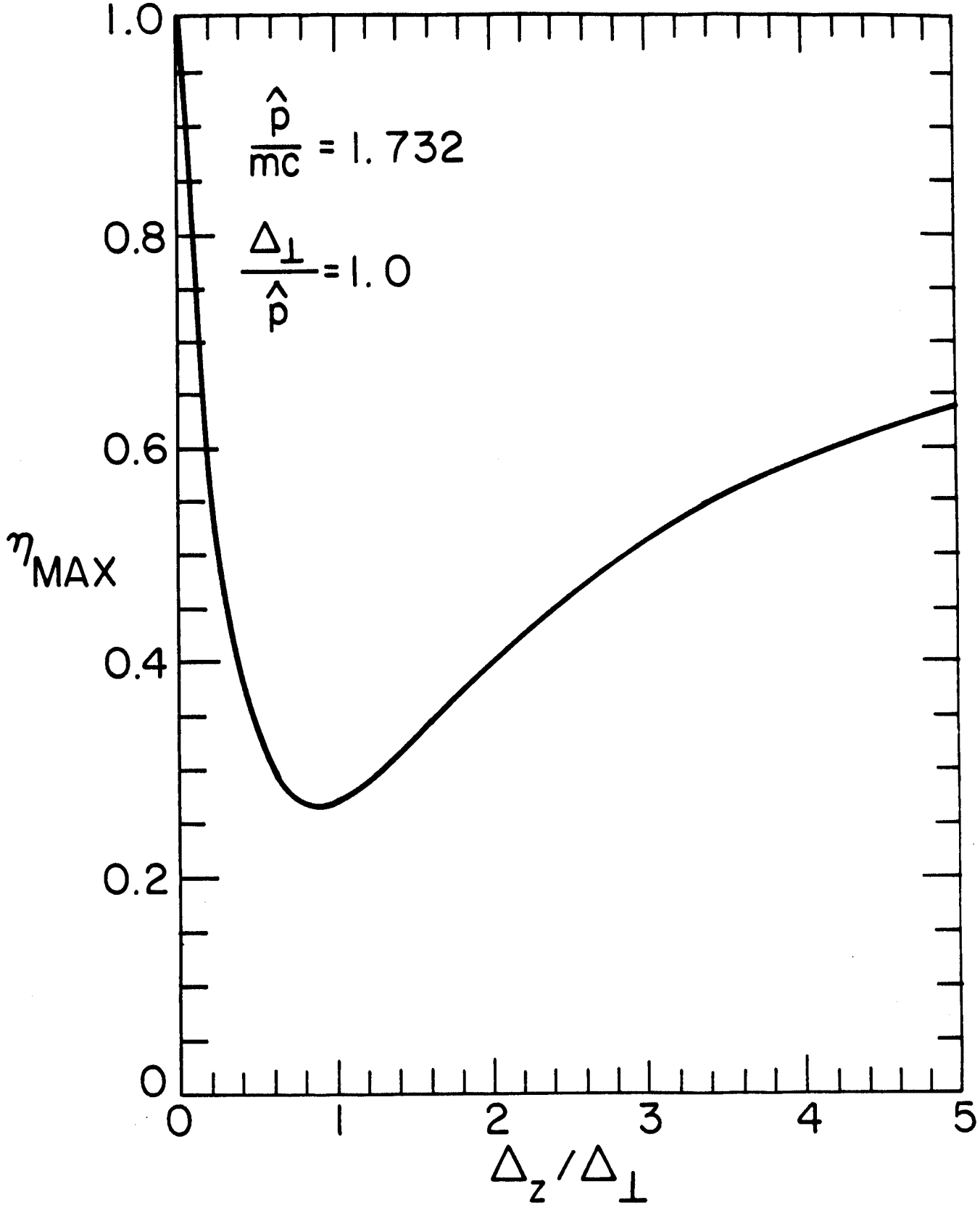
1.0
0.8
0.6
0.4
0.2
0
η_{MAX}
$\frac{\hat{p}}{mc} = 1.732$
$\frac{\Delta_\perp}{\hat{p}} = 1.0$
0
1
2
3
4
5
$\Delta_z/\Delta_\perp$

Fig. 3

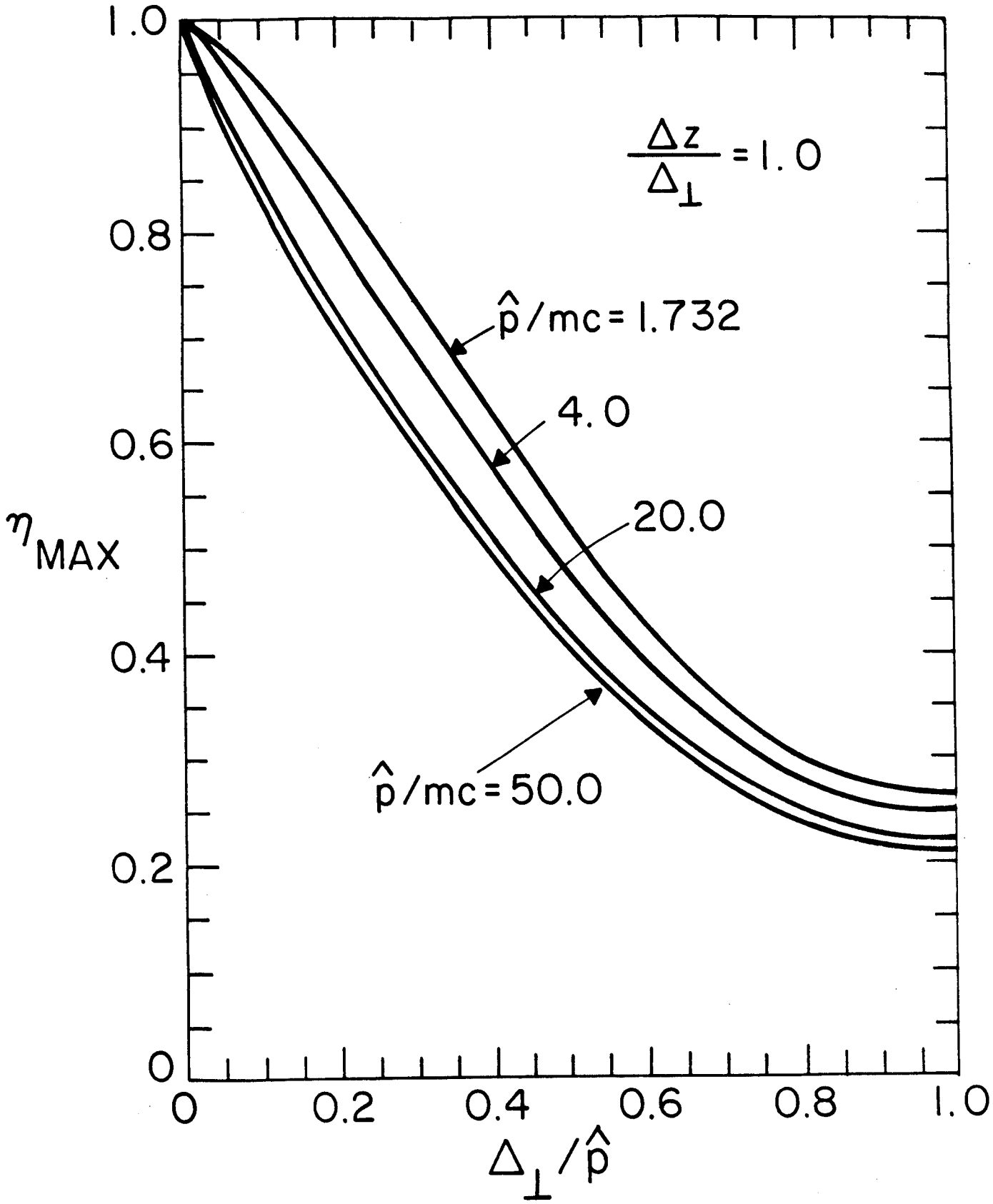
1.0
0.8
0.6
0.4
0.2
0
η_{MAX}
$\frac{\Delta z}{\Delta_\perp} = 1.0$
$\hat{p}/mc = 1.732$
4.0
20.0
$\hat{p}/mc = 50.0$
0
0.2
0.4
0.6
0.8
1.0
$\Delta_\perp/\hat{p}$

Fig. 4

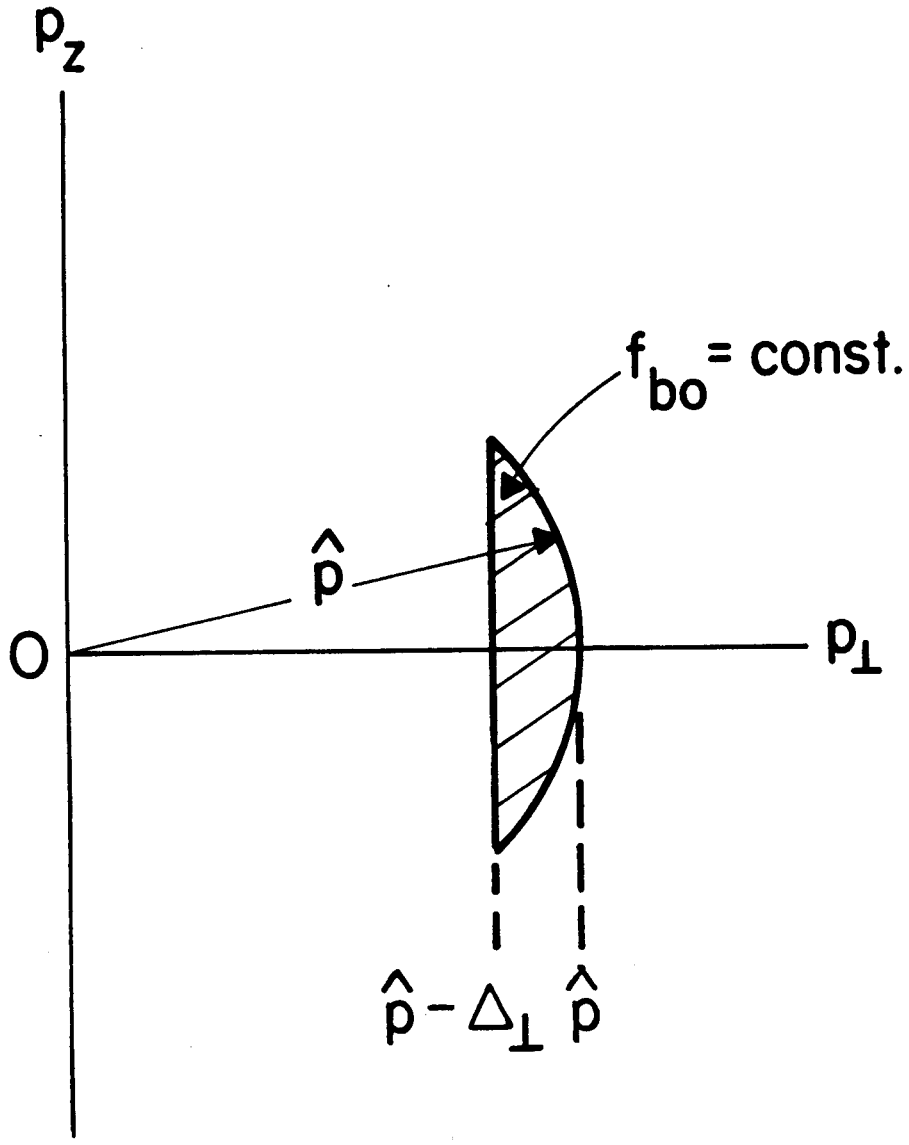

Fig. 5

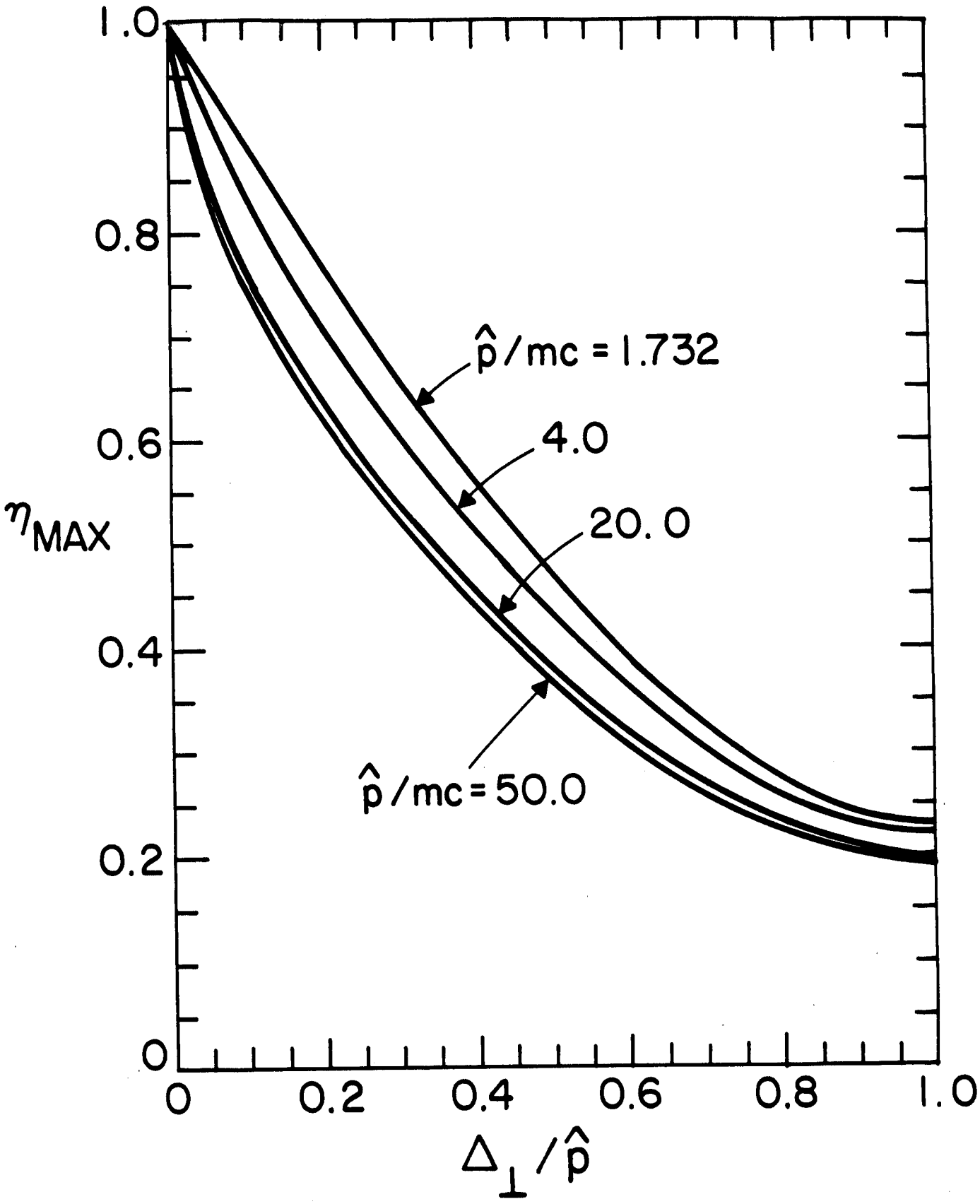
1.0
0.8
0.6
0.4
0.2
0
η_{MAX}
$\hat{p}/mc = 1.732$
4.0
20.0
$\hat{p}/mc = 50.0$
0
0.2
0.4
0.6
0.8
1.0
$\Delta_\perp/\hat{p}$

Fig. 6

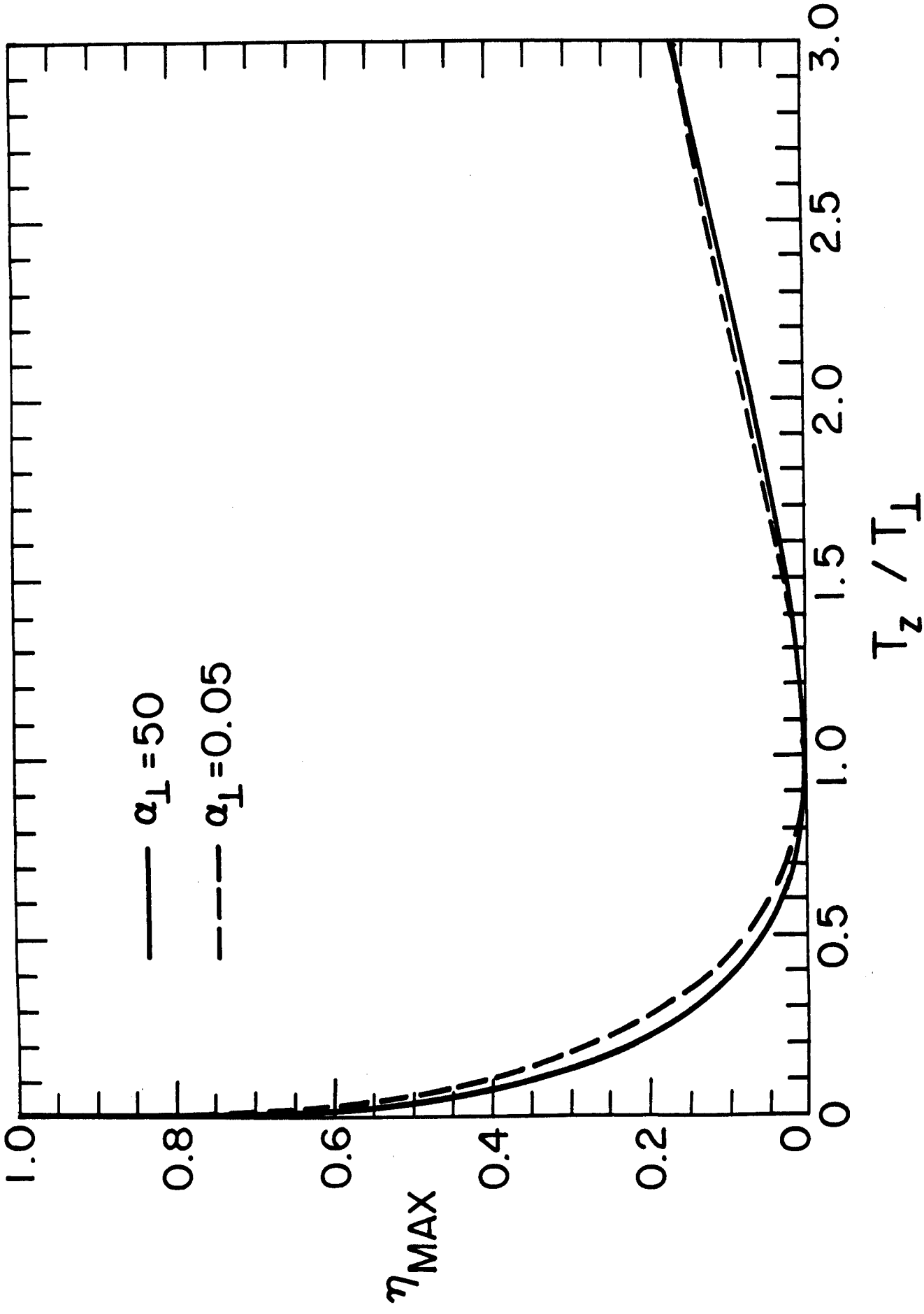
1.0
0.8
0.6
0.4
0.2
0
η_{MAX}
$\alpha_\perp = 50$
$\alpha_\perp = 0.05$
0
0.5
1.0
1.5
2.0
2.5
3.0
$T_z / T_\perp$

Fig. 7